A single radiotracer particle method for the determination of solids circulation rate in interconnected fluidized beds

ELSEVIER

Powder Technology 92 (1997) 53–60

POWDER TECHNOLOGY

A single radiotracer particle method for the determination of solids circulation rate in interconnected fluidized beds

R.D. Abellon [a,*], Z.I. Kolar [a], W. den Hollander [a], J.J.M. de Goeij [a], J.C. Schouten [b], C.M. van den Bleek [b]

[a] *Department of Radiochemistry, Interfaculty Reactor Institute, Delft University of Technology, Mekelweg 15, 2629 JB Delft, Netherlands*

[b] *Department of Chemical Process Technology, Faculty of Chemical Technology and Materials Science, Delft University of Technology, Julianalaan 136, 2628 BL Delft, Netherlands*

Received 18 March 1996; accepted 1 September 1996

Abstract

A non-intrusive method is presented to determine the residence times of a single particle in a facility composed of four interconnected fluidized beds (IFB) with glass beads fluidized by air above minimum fluidization at ambient temperature. It uses a glass particle labelled with radioactive ^{24}Na or ^{192}Ir whose γ-ray emissions are monitored by two external NaI(Tl) scintillation detectors. It is shown that, within the batch particles' size range, the mean residence time of the radiotracer particle is practically independent of the radiotracer particle size and the beds can be considered as practically ideally mixed vessels. It is further demonstrated that the method can adequately measure the residence time distribution of the particles independent of the processes occurring within the system such as the generation of static electricity during fluidization. The presence of static electricity was found to substantially affect the mean residence time of the solids. By relating the bed mass and the mean residence time of the radiotracer particle, the solids circulation rate within the IFB can be obtained.

Keywords: Circulating beds; Fluidized beds; Ionizing radiation; Measurement flow

1. Introduction

Many chemical processes require a stable and continuous circulation of solid particles between reaction compartments. Particularly in the petroleum industry, the development of fluid catalytic cracking represented the first use of solid circulation systems. The key to commercial success of such systems (e.g. Korbee et al. [1]) rests primarily on the design of the solids circulation system; an improper design may result in excessive mechanical damage (attrition) of the solids due to high conveying velocity between the vessels. Several systems have been developed and are discussed extensively elsewhere [2]. Most of them are of the draft-tube type. Some compact forms have been studied such as the four-compartment reactor of Kunii [3]. Other (cold) model systems have also been investigated, namely a fluidized bed connected with a fixed bed via an opening [4], fluidized beds interconnected via submerged orifices and overflow weirs [5,1,6] or an open-loop two compartment circulating system [7,8]. A common problem in all these systems is how to control the solids circulation rate. To find application of any of these systems, the solids and/or gas flows or circulation rates in these systems will have to be predictable and controllable.

The measurement of solids flows or circulation rates underlies many of the experimental studies of dynamic behaviour of gas–solid interconnected beds. Kuramoto et al. [3] measured the solids circulation rate in two ways: (a) by measuring the time taken by the overflowing particles to fill a measuring box attached below the upper edge of the partition plate (an overflow weir); (b) by placing a movable gauze net to catch the overflowing solids at the partition plate and then measuring the time required for the gauze net to pass through a designated distance in the downflowing bed. Ishida and Shirai [4] did not measure solids circulation rate in their apparatus but instead determined the equilibrium bed heights reached when a fluidized bed and a fixed bed are connected through an opening. Yong et al. [5] created a recirculating loop by introducing a fixed rate of solids into the top of the first bed from a hopper by a pulse feeder. The solids flow into the second bed via a submerged orifice and into the third bed via an overflow weir. The solids pass through another submerged orifice into the fourth bed while the overflowing particles in

* Corresponding author. Tel.: +31 15-278 5052; fax: +31 15-278 3906; e-mail: abellon@iri.tudelt.nl

PII S0032-5910(97)03217-8

the fourth bed were collected, weighed and transported back to the hopper above the first bed. Fox et al. [7] had two beds communicating through a rectangular orifice situated at the bottom of a partition plate and the particles flow over a weir in one of the beds. A fixed solids flow rate was fed at the top of the first bed which eventually overflowed at the second bed, while maintaining the bed heights in both beds at the level of the overflow weir. A collecting bucket was placed at the overflow side and the time required to fill this bucket was measured and the mass of the collected solids mass determined.

Mathematical modelling to predict the solids circulation rate in a rig similar to Yong et al. [5] was reported by Korbee et al. [6]. The model calculations were based on the assumption that the determining factor in the solids circulation rate in the IFB is the solids flow through the orifice which is determined by the pressure drop over the orifice. However, there were no experimental data to validate the model calculations. In a more recent work and ensuing the model presented by Fox et al. [7], a mathematical model was presented by Korbee et al. [8] to describe the flow of solids and gas through an orifice between two aerated beds wherein one was operating in a defluidized mode while the other was fully fluidized. The model is based on the forces acting separately in the solid and gas phase and their mutual interactions. The model simulations showed good agreement with experimental data.

This paper describes a non-intrusive, radiotracer-based method to determine the solids circulation rate in a cold, four-cell IFB facility as described by Korbee et al. [6]. This method measures directly the residence times of a single radioactive glass bead (radiotracer particle) in two adjacent cells (beds) in the IFB facility. Lin et al. [9] similarly used a radioactive particle to measure solids motion within a fluidized bed. In our case, the solids circulation rate (F) between the interconnected cells can be determined by using the mean residence time ($\bar{t}$) or MRT of the radiotracer particle and the solids mass (Q) of the pertinent cells. The conditions which underlie this method are: (a) the system must be at steady state; (b) the radiotracer particle and the solids (the tracee) in the cells must be identical in all relevant properties (particle size, shape, density and, probably, electrostatic properties). Further, this paper presents a comparison of the residence time distributions (RTD) of the solid particles with mixing models describing the macroscopic flow patterns occurring within process vessels.

2. Experimental equipment and procedure

2.1. The interconnected fluidized beds (IFB) facility

All experiments were performed under ambient conditions in a facility as shown in Fig. 1. It is a square Perspex column with internal dimensions 0.22 m × 0.22 m and 1.07 m high. It is further divided into four square cells using 20 mm thick divider plates. Each cell has an effective dimension of 0.1 m width, 0.1 m length and 1 m height. At the bottom of the column are windboxes and gas distributors for each cell. Separating the cells from the windboxes are 3 mm thick porous sintered bronze plates (Poral BK4-30-30 type, France) to distribute air through the cells. The column as a whole is mounted on a steel frame for easy transport. Fig. 2 is a cross section of the column at the orifice level. The partition plate separating cells b and c (and d and a) is 20 mm thick and 0.3 m high. The top of the plate serves as a rectangular overflow weir during fluidization. To prevent deposition of solid material, the face of the weir is sharpened at the mid-line with a 20° slope at each side.

In the partition plate dividing cells a and b (and cells c and d) is a 70 mm diameter circular opening with centre 45 mm above the bronze plate. Into this opening, an orifice plug (20 mm thick) with a built-in orifice can be fitted. At the outer cell walls, right opposite the orifice plug, are pressure taps where probes can be introduced. These probes measure the pressure in the cells or the pressure drop across the orifices. They are made of stainless steel pipes (about 4 mm i.d.) with perspex end pieces terminated with fine-wire gauze at the gauging end to prevent the entry of solid particles into the pipes.

Cells a and d and cells b and c are joined together via the orifice plugs. Several orifice plugs can therefore be used to vary the orifice opening. The cells are finally pinned at the top and at the sides by clips to fully assemble the facility. Thus, cell a is connected to cell b via an orifice, cell b to cell c via an overflow weir, cell c to cell d via an orifice and finally cell d to cell a via an overflow weir. In this manner, a completely recirculating IFB system is realized.

2.2. Solid particles and characterization

There were two batches of glass beads used (Dragonit 25, lead-free, Rowa Techniek, Netherlands), hereafter called Batch 1 and Batch 2. Particle characterization was performed by first collecting about 50 g of sample from a 25 kg bulk material using a spinning riffler (Retsch Laboratory Sample Divider Type PT, Germany). Particle sizing was done using an image analyzer (Magiscan 2A, Joyce Loebl, UK). Table 1 shows the measured particle size ranges, average particle diameter $\bar{d}_p$, average batch circularity from about 600 particles per batch [10] and the particle density. From the circularity measurements and optical observations, it was obvious that the glass beads were essentially spherical particles. Hence, a sphericity ψ equal to 1 was used in the estimation of the minimum fluidization velocity. In powder technology practice, the surface-volume diameter d_{sv} is the standard diameter definition [11]. This was determined for each batch and was found to deviate only by 1% from the average particle diameter $\bar{d}_p$. Consequently, d_{sv} is equal to $\bar{d}_p$. Finally, the density of the particles ρ_p (sample mass used: 30–80 g) was measured by water displacement pycnometry.

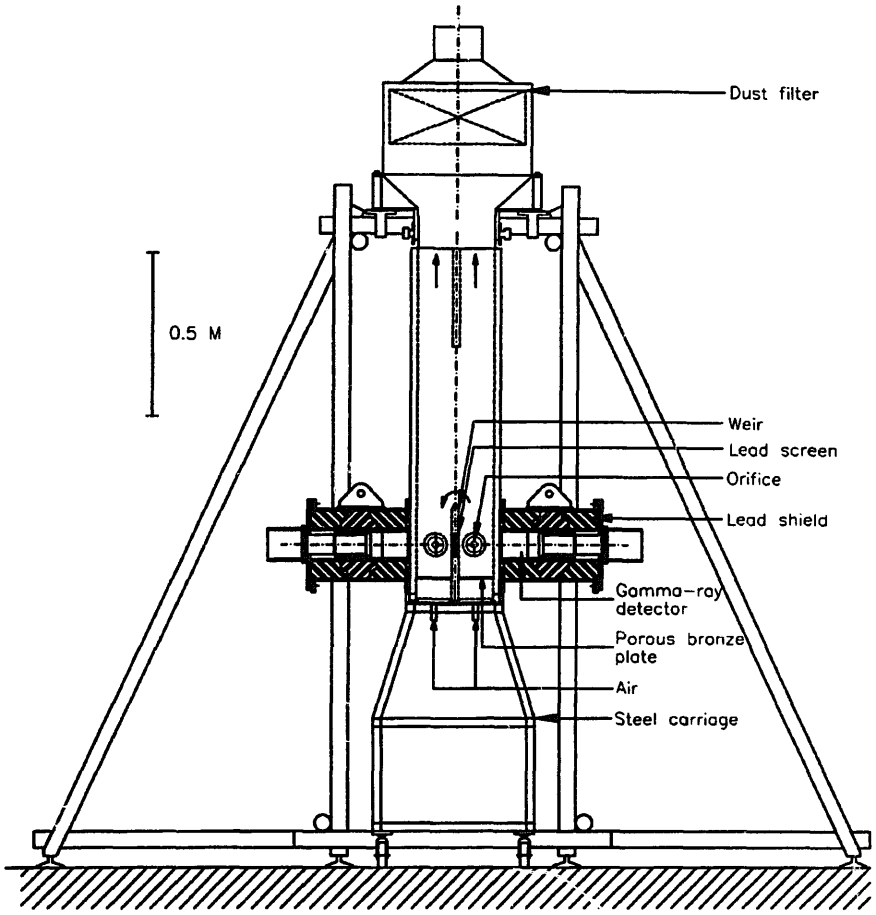

Fig. 1. The interconnected fluidized beds (IFB) facility.

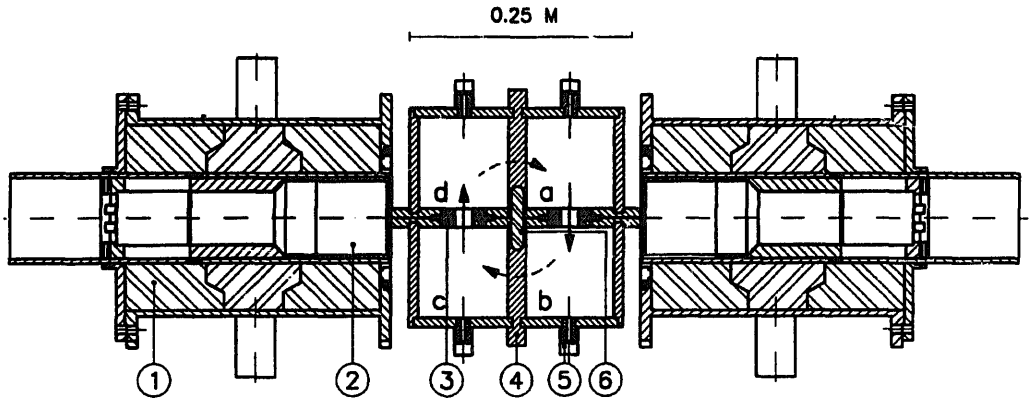

Fig. 2. Cross section of the IFB facility at the orifice level: (1) lead shield, (2) gamma-ray detector, (3) orifice plug, (4) perspex wall, (5) pressure probe tap, (6) lead screen.

Table 1
The particles characterization of Batch 1 and Batch 2 using image analysis and pycnometry (average ± standard deviation)

Parameter	Batch 1	Batch 2
Size range (μm)	460–916	472–728
Average diameter, $\bar{d}_p$ (μm)	662 ± 70	594 ± 52
Average density, ρ_p (kg m^{-3})	2572 ± 10	2568 ± 32
Average circularity (–)	0.99 ± 0.02	0.97 ± 0.02

Fig. 3 shows the particle size distributions of Batch 1 ($\bar{d}_p$ = 662 μm) and Batch 2 ($\bar{d}_p$ = 594 μm).

2.3. Fluidizing gas

Air flow was supplied at 600 kPa from a central air compressor and conditioner giving a dew point of 4°C. It was subsequently measured and controlled using four mass flow meters/controllers (EL-Flow model F-203C, Bronkhorst Hi-

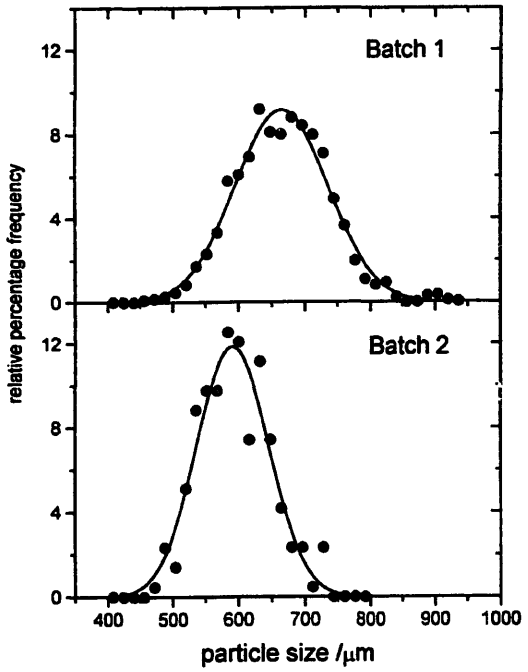

Fig. 3. Particles size distribution of Batch 1 and Batch 2.

Tec, Netherlands) and was led to the four windboxes and gas distributors. Effluent air from each cell was passed through a dust filter (see Fig. 1) whereby entrained powders were filtered out. Composite air temperature was measured, at the top of the IFB, using an iron-constantan thermocouple and averaged over the experimental duration. A precision barometer was used to measure atmospheric pressure. Air temperature and atmospheric pressure were necessary to determine the (superficial) fluidization velocities in the cells. Friction between the glass particles, friction between particles and the cell walls and the dry fluidizing air led to the generation of static electricity. As the relative humidity of the central air supply had to be kept low for other users, static electricity in the IFB was suppressed by the addition of NaCl powder into the fluidized beds.

2.4. Minimum fluidization velocity

The minimum fluidization velocity U_{mf} was experimentally determined and compared to those predicted by known correlations [12,13]. This was done by filling the column with glass beads to 0.2 m height and then fluidizing the beads. Air supply was then reduced in a stepwise fashion to zero while the pressure drop across the bed was measured for each step using a water manometer. This was done several times and from the air mass flow rate versus pressure drop curve produced, the U_{mf} was determined. For Batch 1 having an average particle size $\bar{d}_p$ of 662 μm, the experimental U_{mf} was 0.32 ± 0.01 m s^{-1} while Wen and Yu [12] would predict 0.31 m s^{-1} and Chitester et al. [13] 0.40 m s^{-1}; for Batch 2, where $\bar{d}_p$ was 594 μm, the experimental U_{mf} was also 0.32 ± 0.01 m s^{-1} while Wen and Yu [12] would predict 0.26 m s^{-1} and Chitester et al. [13] 0.34 m s^{-1}. For classification purposes, the glass beads used were considered Geldart B particles [14].

2.5. Radiotracer

The best radiotracer for the glass beads is a glass bead having identical properties except that it contains a radionuclide that emits ionizing radiation. This radiation must be detectable at the outer side of the apparatus so as not to disturb the prevailing fluidization conditions. Dragonit 25 glass contains, among others, about 7% by weight Na. Sodium when irradiated with thermal neutrons in a nuclear reactor produces radioactive ^{24}Na according to the reaction ^{23}Na$(n,\gamma)^{24}$Na. The radionuclide ^{24}Na decays with a half-life of 15.02 h to stable ^{24}Mg by emitting beta-particles of $E_{max} = 1.389$ MeV (100%) and γ-rays of 1.368 (100%) and 2.754 (100%) MeV [15].

As the bed particles were not monodisperse, the radiotracer particle size was varied to investigate the relation between the radiotracer particle size and its MRT with all other system parameters kept constant. The radiotracer particles were selected from the two batches within their respective size ranges.

Another radiotracer particle was produced by making a melt of glass by adding up to 0.05% iridium (by weight). Iridium was chosen due to its very high (n,γ) reaction cross section, i.e. the probability that its nucleus will react to an impinging neutron is very high and this facilitates activation. The percentage of iridium added must be kept low as the density of the produced glass should not deviate significantly from the glass bead density. From the cold melt, lumps were shaped into spheres of desired diameters. These spheres were then irradiated with thermal neutrons to produce, among others, radioactive ^{192}Ir which decays with a half-life of 74.2 days to stable ^{192}Pt by emitting beta-particles of $E_{max} = 0.672$ (46.4%), 0.536 (41.4%), 0.240 (8.2%) MeV and γ-rays of primarily 0.316 (100%) MeV [15]. Owing to the long half-life of ^{192}Ir, the iridium-labelled particles are very useful when testing the reproducibility of experiments as it can be used over and over again.

The radioactivity produced is dependent on the components present and their concentration levels, the particle size, the thermal neutron flux and irradiation duration. For instance, a sodium containing particle of 600 μm diameter produced a ^{24}Na activity of about 1 MBq after 24 h of irradiation with a thermal neutron flux of 6×10^{16} m^{-2} s^{-1} and a cooling time of 4 h. Likewise, an iridium containing particle of the same size produced an ^{192}Ir activity of about 6 MBq after 24 days of irradiation with a thermal neutron flux of 2×10^{18} m^{-2} s^{-1} and a cooling time of 5 days.

2.6. Radiometry

The γ-rays emitted by the above-mentioned radionuclides can be detected easily by detectors placed outside the apparatus. Two external, lead-shielded 2″×2″ NaI (Tl) scintil-

lation detectors (Quartz and Silice, Type 51SEA76, France) were used to measure the intensity of the γ-rays emitted by the radiotracer particle as it moved within the cells. Both detectors were connected to corresponding amplifier/single channel analyzers (Canberra model 20151A, USA) and a multichannel data processor. Detector 1 was positioned against the walls of cells a and b while detector 2 was focused on cells c and d. Fig. 2 shows the arrangement of the detectors with respect to the IFB facility. The two detectors were started simultaneously. As the radiotracer particle moved in and through the four cells, the intensity of the γ-rays detected would vary. Intensity variation is due to the fluctuating distance of the mobile radiotracer particle with respect to the detector thus causing varying attenuation of γ-rays. Signals from the two detectors are therefore complementary as the radiotracer particle could only be in one location at any given time: either closer to detector 1 and farther from detector 2 or otherwise. The chance that the radiotracer stayed stationary in the middle is practically nil. The γ-ray energy regions chosen in all runs were around 1.3 MeV for ^{24}Na-labelled particles and around 0.3 MeV for ^{192}Ir-labelled particles.

A dedicated PC-based data acquisition system was designed and built to set, control and store radiometric and process conditions data in the facility. All measurements were constantly displayed on the PC monitor. Fluidization air mass flow rates were read and controlled every 10 s. The detectors integrated the radiation intensity (counts) during a specified time interval called dwell time. This dwell time was varied from 1 to 5 s. The counts collected were then stored in 2048 channels, one channel per dwell time. When all the channels were used, the stored data were subsequently corrected for radioactive decay, smoothed, if desired, and finally transferred to the hard disk or to a floppy diskette. A 'refreshed' display would appear as soon as all the data had been transferred. Depending on the activity of the radiotracer particle, one run could last up to 5 days.

2.7. Calculations

In a steady state system, the solids circulation rate (F) can be calculated provided the mass (Q) and the mean residence time (MRT) of the solid particles in the cells ($\bar{t}$) are known. Thus,

$$F = Q/\bar{t} \tag{1}$$

If all flowing particles were of identical properties (monodisperse size, density, shape, etc.), then the MRT of all the particles ($\bar{t}$) is the same as the MRT of a single particle ($\bar{t}_{sp}$). In that case, a labelled particle (tracer) should have the same MRT as any individual particle (tracee) in the system. Similarly, a glass bead labelled with a radionuclide (radiotracer particle) will have the same MRT as the other glass beads ($\bar{t}_{radiotracer}$). Hence,

$$\bar{t}_{radiotracer} = \Sigma t_{i,radiotracer}/n = \bar{t}_{sp} = \bar{t} \tag{2}$$

and

$$\sigma_{radiotracer} = [\Sigma(t_{i,radiotracer} - \bar{t}_{radiotracer})^2/(n-1)]^{1/2} = \sigma_{sp} = \sigma \tag{3}$$

where $t_{i,radiotracer}$ is the measured residence time of the radiotracer particle, n is the number of (half-cycle) measurements and σ is the corresponding standard deviation. The relative standard error, ϵ, can be calculated using

$$\epsilon = 100 \times \sigma/(\bar{t}\sqrt{n}) \tag{4}$$

By choosing an adequate number of measurements n, one can limit ϵ to about 5%.

The measured $\bar{t}$ and its variance (σ^2) can be used to calculate N_{exp} (the number of tanks in series) by using [16]

$$N_{exp} = \bar{t}^2/\sigma^2 \tag{5}$$

Thus from the experimental RTD N_{exp} can be estimated.

On the other hand, the RTD of the solid particles can also be described mathematically by the gamma-function model [17]

$$f(t) = N^N t^{N-1} \exp - (N \times t/\bar{t})/[\bar{t}^N \times \Gamma(N)] \tag{6}$$

where N is the number of mixed tanks in series and $\Gamma(N)$ is the gamma-function defined as ${}_0\int^\infty \epsilon \exp(-x)\, x^{N-1}\, dx$ and is equal to $(N-1)!$ when N is a positive integer. By fitting this function into the experimental RTD, one can estimate N ($=N_{fit}$).

The adequacy of the experimental method can be substantiated when the estimated N_{fit} shows good agreement with the experimental N_{exp}.

2.8. Experimental procedure

The IFB facility was filled with 12 kg of glass beads. Batch 1 was fluidized as is, while about 15 g of NaCl powder were added to Batch 2 to 'reduce' static electricity. Cells a and c were fluidized at 1.3 times U_{mf} while cells b and d were fluidized at 2 times U_{mf}. The orifice used for this study had a 15 mm diameter. The cells were fluidized for at least 15 min to achieve steady state conditions. This duration was experimentally determined by stopping the air flow abruptly at a certain time and by weighing the contents of the two cells. The shortest time during which the cells mass attained a constant value was found to be about 15 min. The radiotracer particle was then introduced into cell a. Automatic data acquisition was triggered at the moment the radiotracer particle re-enters cell a. For this study, an 11-point smoothing (by moving average) of the detector signals was arbitrarily chosen. The number of points used (period) and number of times smoothing is performed must always reflect the sharp transitions when the radiotracer particle leaves the vicinity of one detector, via the overflow weir, and comes closer to the other detector. The radiotracer particle size was subsequently varied while maintaining the same solids population and the same fluidization regimes in the cells. This procedure was performed for both Batch 1 and Batch 2.

To test the reproducibility of the experimental results, an iridium-containing particle was used. This had a particle size of 595 μm. There were two runs for each batch. All process conditions were identical, fluidization was started with a freshly cleaned IFB and a 5 day interval between each run.

In all the procedures described above, solids flow was in the clockwise direction. In order to ascertain that the measured RTD is not influenced by possible structural asymmetry in the IFB facility (wall roughness, gas distribution, etc.), the solids flow direction was reversed. This was done by changing the sequence of the fluidization regimes in the cells: counterclockwise flow meant cells a and c being fluidized at $2 \times U_{mf}$ and cells b and d at $1.3 \times U_{mf}$.

3. Results and discussion

3.1. Ambient conditions and detector response

Average air temperature ranged from 19 to 23°C and the atmospheric pressure ranged from 1010 to 1030 hPa (mbar). Fig. 4 shows typical raw and smoothed responses (collected counting rates) by both detectors during the preliminary runs. It was apparent from these runs that detector responses were complementary to each other and smoothing the responses once was adequate to characterize the movement of the radiotracer particle in the IFB. Fig. 4 shows that one 'block width' of high counting rates in one detector (or one 'block width' of low counting rates in the other) corresponds to one residence time of the radiotracer particle.

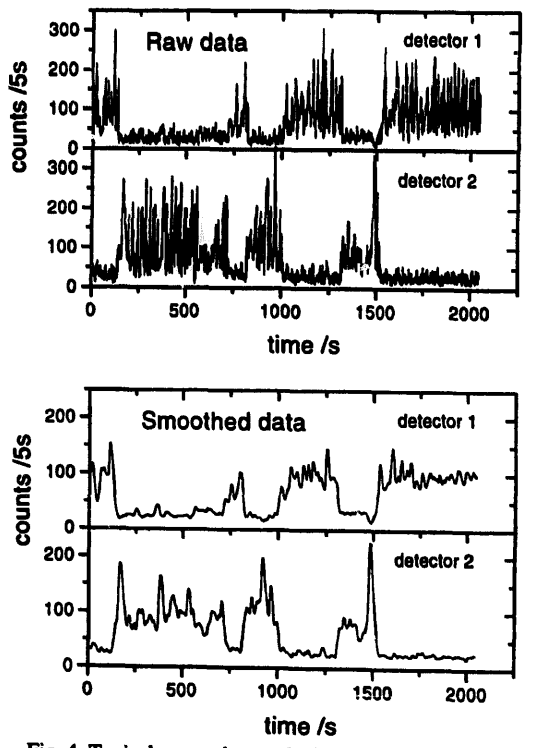

Fig. 4. Typical raw and smoothed detectors' responses.

3.2. Mean residence time (MRT)

Illustrative examples of the results of experiments is shown in Fig. 5. From the 'block widths' or residence times, $\bar{t}_{radiotracer}$ and $\sigma_{radiotracer}$ were calculated using Eqs. (2) and (3). The relationship between $\bar{t}_{radiotracer}$ and the radiotracer particle size used is shown in Fig. 6. It is evident that $\bar{t}_{radiotracer}$ in the two cells is about (a) 430 s for Batch 1 and (b) 230 s for Batch 2. These indicate that $\bar{t}_{radiotracer}$ is practically independent of the radiotracer particle size, provided it is within the batch's size range. This means that all particles are fluidized and behave as one 'homogeneous fluid' flowing from one cell to another. Therefore, the assumption that $\bar{t}_{radiotracer}$ is equal to $\bar{t}$ is validated.

From the radiometric point of view, it follows further that any particle size, within the solid particles' size range, can be used as radiotracer particle. However, a large particle size is preferred as it offers the benefit of higher yield of thermal neutron activation. It can then be used for longer periods of time depending on the half-life of the relevant radionuclide label.

On the other hand, one will note $\bar{t}$ of Batch 1 is almost twice as large as that of Batch 2. The only evident differences between the two batches were the absence of static electricity in Batch 2 and the somewhat dissimilar particles size distribution. To be sure, an extra experiment on Batch 1 was performed right after unloading Batch 2 from the IFB, without cleaning it, and residence time of a radiotracer particle with a diameter of about 600 μm measured. This resulted to a $\bar{t}$ of 500 s and, again, an obvious presence of static electricity. Moreover, neutron activation analysis of the solid particles

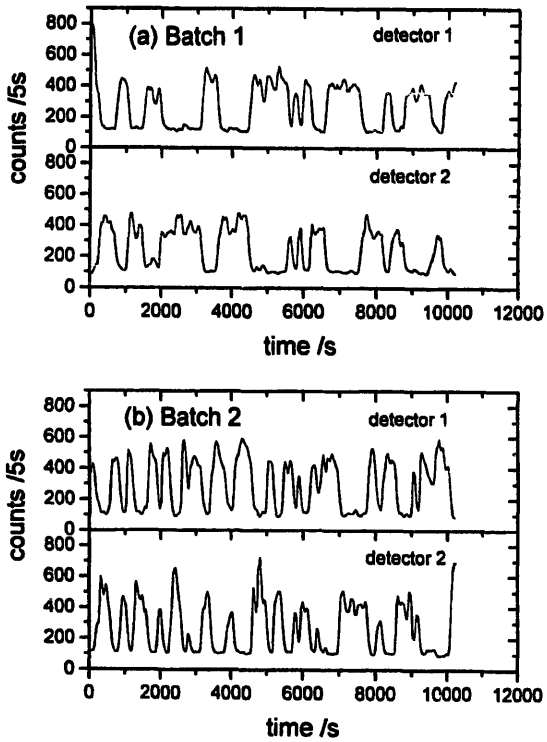

Fig. 5. Illustrative experimental results: (a) Batch 1 ($\bar{t}$ = 449 s, σ = 330 s); (b) Batch 2 ($\bar{t}$ = 245 s, σ = 176 s).

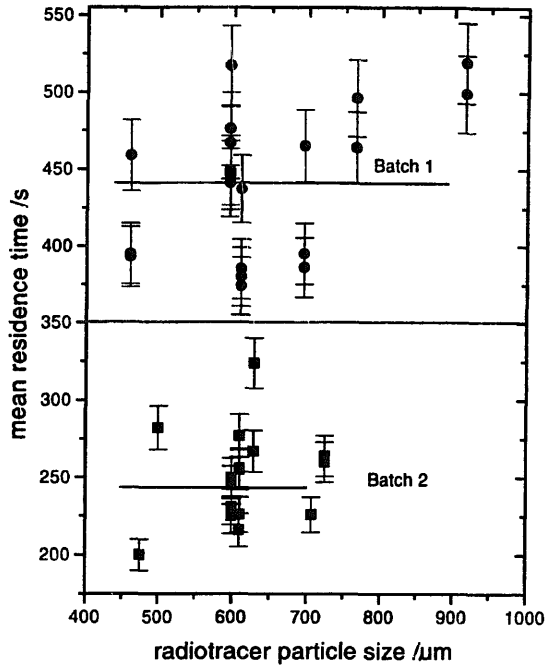

Fig. 6. Radiotracer particle size vs. mean residence time. Points indicate $\bar{t}_{\text{radiotracer}} \pm$ standard error ($= \sigma/\sqrt{n}$). Horizontal lines indicate the particle size ranges and the average values for Batch 1 (about 430 s) and Batch 2 (about 230 s).

of both batches showed no significant difference in chemical composition. This leaves one to conclude that the particle size distribution and the static electricity production in the IFB substantially influence the MRT of the solid particles. The influence of static electricity on the dynamics and rheology of fluidized beds was discussed by Wolny and Kazmierczak [18]. They concluded that electrification of fluidized beds causes particle agglomeration, bed porosity increase and micro-chanelling, among others. These phenomena affect the rheology of the system thus exhibiting non-Newtonian fluid characteristics in the emulsion phase and for some air velocity ranges, pseudoplastic fluid properties. Increasing the relative humidity of air up to 70% or the addition of fines (NaCl or Al) was found to neutralize static electricity.

3.3. Experimental reproducibility and flow direction effect

Table 2 reports the results of reproducibility runs and the effect of changing the flow direction. It is shown here that using the single radiotracer particle method, experimental results are reproducible for both batches and $\bar{t}$ is independent of the flow direction.

Table 2
Reproducibility of experimental results and the effect of varying the flow direction on the measured mean residence time (s). Radiotracer particle used: ^{192}Ir-labelled glass bead. Values are expressed as mean ± standard deviation

Run	Reproducibility		Flow direction (Batch 2)	
	Batch 1	Batch 2	Clockwise	Counterclockwise
1	385 ± 296	218 ± 150	225 ± 162	231 ± 156
2	380 ± 273	226 ± 161		

3.4. Solids circulation rate

It has been shown that the radiotracer method is suitable to measure the MRT of the solid particles in the IFB. Using the MRT of the radiotracer particle, the solids circulation rate (F) can be calculated (Eq. (1)). At steady state, the mass content of the two cells was 6 kg. Thus, F is about 13 g s^{-1} for Batch 1 and about 24 g s^{-1} for Batch 2, or 73 and 136 kg s^{-1} m^{-2} of orifice area, respectively.

3.5. Mixing patterns in the IFB

Typical experimental RTDs are shown in Fig. 7 for Batch 1 and Batch 2. From the calculated $\bar{t}$ and σ, N_{exp} was calculated using Eq. (5) for these runs. These values were then compared to N_{fit} derived by fitting a gamma-function model into the experimental RTDs. The software STATGRAPHICS 5.1 (STSC Inc., USA) was used for this purpose, where the gamma-function is expressed as

$$f(t) = \beta^{\alpha} t^{\alpha-1} \exp(-\beta t)/\Gamma(\alpha) \qquad (7)$$

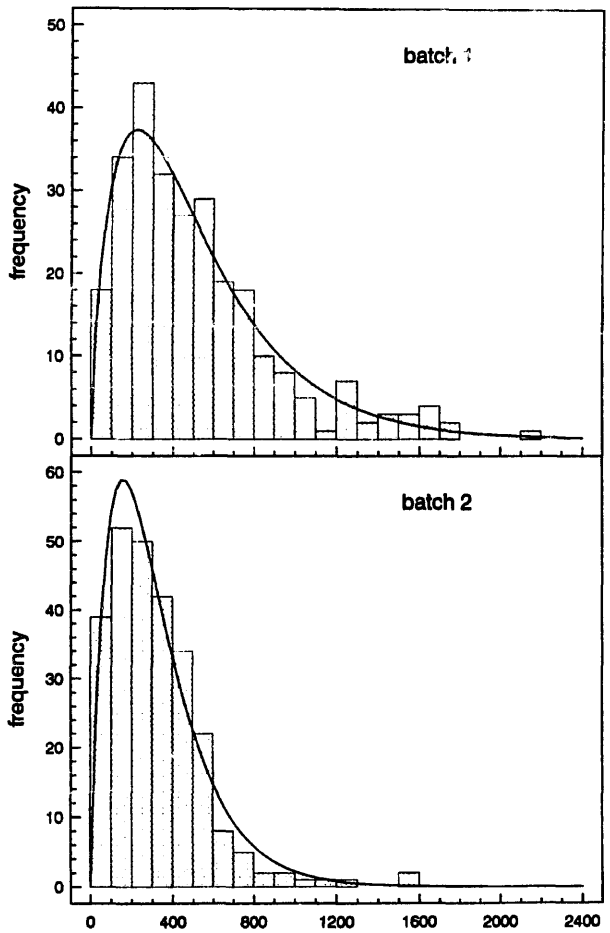

Fig. 7. The experimental residence time distributions and the fitted gamma-functions (Eq. (7)) for Batch 1 and Batch 2.

Table 3
Illustrative experimental results comparing N_{exp} (Eq. (5)) and N_{fit} (Eq. (7)). Radiotracer particle used: ^{24}Na-labelled glass bead

Parameters	Batch 1	Batch 2
n	268	261
$\bar{t}$ (s)	517	324
σ (s)	387	237
ϵ (%)	4.6	4.5
N_{exp}	1.78	1.87
α	1.763	1.915
β (s^{-1})	0.0034	0.0059
N_{fit}	1.76	1.92

Since Eqs. (6) and (7) are equal, the shape parameter α is therefore equal to N_{fit} and the scale parameter β is equal to $(N/\bar{t})_{fit}$. The values of α and β were calculated to give the best fit, by least sum of squares method. Table 3 summarizes the results of the curve fittings and calculations using Eq. (5). This is graphically illustrated in Fig. 7 which shows the experimental RTDs and the fitted gamma-functions for both batches.

From these results, N_{fit} was found to be only 5–10% off the value of two ideally mixed tanks. This means that the IFB operating under these particular fluidization regimes can be considered essentially as ideally mixed tanks or vessels.

4. Conclusions

It is shown above that the single radiotracer particle approach is a suitable method to quantify the solids circulation rate in the IFB system without disturbing the internal conditions of the system. The method demonstrates its independence from the prevailing conditions within the system being studied. It was found using this method that, within the batch's particle size range, the mean residence time of the radiotracer particle is independent of the radiotracer particle size.

Therefore, it can be concluded that: (a) all fluidized particles have practically the same $\bar{t}$; (b) the IFB operating under the above-mentioned regimes can be considered as ideally mixed tanks; (c) the presence of static electricity in fluidized beds influences the residence time distribution of the solid particles.

The method described above will be used in further investigations of solids flow in the IFB in relation to both bed properties and fluidization regimes.

5. List of symbols

$\bar{d}_p$	average particle diameter (μm)
d_{sv}	surface/volume particle diameter (μm)
E	radiation energy (MeV)
F	solids circulation (or flow) rate (kg s^{-1})
n	number of residence time measurements
N	number of tanks in series
Q	quantity of solids (kg)
$\bar{t}$	mean residence time (MRT) of solid particles (s)
t_i	residence time of the radiotracer (s)
$\bar{t}_{radiotracer}$	MRT of the radiotracer particle (s)
$\bar{t}_{sp}$	MRT of a single particle (s)
U_{mf}	minimum fluidization velocity (m s^{-1})

Greek letters

α	shape (fit)-parameter in Eq. (7)
β	scale (fit)-parameter in Eq. (7)
$\Gamma(\alpha)$	gamma-function of α
γ	gamma-ray
ϵ	relative standard error (%)
ρ	particle density (kg m^{-3})
σ	standard deviation (s)
ψ	particle sphericity

Acknowledgements

The authors are grateful for the assistance of Mgr Ing Z.R. Dziewonski in the realization of the process control and data acquisition system and to Ms T. Verburg for the generous computer assistance.

References

[1] R. Korbee, J. Grievink, J.C. Schouten and C.M. van den Bleek, *Proc. Int. Conf. Fluidized Bed Combustion*, Vol. 2, ASME, New York, 1993, p. 1143.
[2] D. Kunii and O. Levenspiel, *Fluidization Engineering*, Butterworth-Heinemann, Boston, MA, 2nd edn., 1991, p. 359.
[3] M. Kuramoto, T. Furusawa and D. Kunii, *Powder Technol., 44* (1985) 77.
[4] M. Ishida and T. Shirai, *J. Chem. Eng. Jpn., 9* (1976) 249.
[5] J. Yong, W. Zhahwen, Z. Jingxu and Y. Zhiqing, *Conf. Papers, Second China–Japan Symp., Kunming, 1985*, p. 172.
[6] R. Korbee, J.C. Schouten and C.M. van den Bleek, *AIChE Symp. Ser., 87* (1991) 70.
[7] D. Fox, Y. Molodtsof and J.F. Large, *AIChE J., 35* (1989) 1933.
[8] R. Korbee, O.C. Snip, J.C. Schouten and C.M. van den Bleek, *Chem. Eng. Sci., 49* (24B) (1994) 5819.
[9] J.S. Lin, M.M. Chen and B.T. Chao, *AIChE J., 31* (1985) 465.
[10] T. Allen, *Particle Size Measurement*, Chapman and Hall, London, 3rd edn., 1985, p. 210.
[11] D. Geldart, in D. Geldart (ed.), *Gas Fluidization Technology*, Wiley, Chichester, UK, 1986, pp. 11–16.
[12] C.Y. Wen and Y.H. Yu, *AIChE J., 12* (1966) 610.
[13] D.C. Chitester, R.M. Kornosky, L.S. Fan and J.P. Danko, *Chem. Eng. Sci., 39* (1984) 253.
[14] D. Geldart, *Powder Technol., 7* (1973) 285.
[15] C.M. Lederer and V.S. Shirley, *Table of Isotopes*, Wiley, New York, 7th edn., 1978, p. 42 and 1229.
[16] O. Levenspiel, *Chemical Reaction Engineering*, Wiley, New York, 2nd edn., 1972, pp. 290–293.
[17] E.B. Nauman and B.A. Buffham, *Mixing in Continuous Flow Systems*, Wiley, New York, 1983, pp. 60–64.
[18] A. Wolny and W. Kazmierczak, *Chem. Eng. Sci., 48* (1993) 3529.